


Chemotherapy impairs skeletal muscle mitochondrial homeostasis in early breast cancer patients

Joris Mallard^{1,2,3}, Elyse Hucteau^{1,2,3}, Anne-Laure Charles¹, Laura Bender³, Claire Baeza³, Mathilde Pélissie³, Philippe Trenszt³, Carole Pflumio³, Michal Kalish-Weindling³, Bernard Gény^{1,2}, Roland Schott³, Fabrice Favret^{1,2}, Xavier Pivot³, Thomas J. Hureau^{1,2} & Allan F. Pagano^{1,2*} 

¹Faculté de médecine, maïeutique et sciences de la santé, “Mitochondrie, Stress oxydant, Protection musculaire”, Université de Strasbourg, Strasbourg, France; ²Faculté des Sciences du Sport, Centre Européen d’Enseignement de Recherche et d’Innovation en Physiologie de l’Exercice (CEERIPE), Université de Strasbourg, Strasbourg, France; ³Institut de Cancérologie Strasbourg Europe (ICANS), Strasbourg, France

Abstract

Background Chemotherapy is extensively used to treat breast cancer and is associated with skeletal muscle deconditioning, which is known to reduce patients’ quality of life, treatment efficiency, and overall survival. To date, skeletal muscle mitochondrial alterations represent a major aspect explored in breast cancer patients; nevertheless, the cellular mechanisms remain relatively unknown. This study was dedicated to investigating overall skeletal muscle mitochondrial homeostasis in early breast cancer patients undergoing chemotherapy, including mitochondrial quantity, function, and dynamics.

Methods Women undergoing (neo)adjuvant anthracycline-cyclophosphamide and taxane-based chemotherapy participated in this study (56 ± 12 years). Two muscle biopsies were collected from the vastus lateralis muscle before the first and after the last chemotherapy administration. Mitochondrial respiratory capacity, reactive oxygen species production, and western blotting analyses were performed.

Results Among the 11 patients, we found a decrease in key markers of mitochondrial quantity, reaching –52.0% for citrate synthase protein levels ($P = 0.02$) and –38.2% for VDAC protein levels ($P = 0.04$). This mitochondrial content loss is likely explained by reduced mitochondrial biogenesis, as evidenced by a decrease in PGC-1 α 1 protein levels (–29.5%; $P = 0.04$). Mitochondrial dynamics were altered, as documented by a decrease in MFN2 protein expression (–33.4%; $P = 0.01$), a key marker of mitochondrial outer membrane fusion. Mitochondrial fission is a prerequisite for mitophagy activation, and no variation was found in either key markers of mitochondrial fission (Fis1 and DRP1) or mitophagy (Parkin, PINK1, and Mul1). Two contradictory hypotheses arise from these results: defective mitophagy, which probably increases the number of damaged and fragmented mitochondria, or a relative increase in mitophagy through elevated mitophagic potential (Parkin/VDAC ratio; +176.4%; $P < 0.02$). Despite no change in mitochondrial respiratory capacity and COX IV protein levels, we found an elevation in H₂O₂ production ($P < 0.05$ for all substrate additions) without change in antioxidant enzymes. We investigated the apoptosis pathway and found an increase in the protein expression of the apoptosis initiation marker Bax (+72.0%; $P = 0.04$), without variation in the anti-apoptotic protein Bcl-2.

Conclusions This study demonstrated major mitochondrial alterations subsequent to chemotherapy in early breast cancer patients: (i) a striking reduction in mitochondrial biogenesis, (ii) altered mitochondrial dynamics and potential mitophagy defects, (iii) exacerbated H₂O₂ production, and (iv) increased initiation of apoptosis. All of these alterations likely explain, at least in part, the high prevalence of skeletal muscle and cardiorespiratory deconditioning classically observed in breast cancer patients.

Keywords Mitochondrial biogenesis; Mitochondrial dynamics; Apoptosis; Skeletal muscle deconditioning; Mitophagy; H₂O₂

Received: 13 October 2021; Revised: 22 February 2022; Accepted: 7 March 2022

*Correspondence to: Allan F. Pagano, Faculté des Sciences du Sport, Centre Européen d’Enseignement de Recherche et d’Innovation en Physiologie de l’Exercice (CEERIPE), Université de Strasbourg, 14 rue René Descartes, 67084 Strasbourg, France. Phone: 03 68 85 60 44, Email: allan.pagano@unistra.fr

Introduction

Anthracycline/cyclophosphamide-based and taxane-based chemotherapies (CT) are commonly administered as (neo)adjuvant therapies to treat patients with early breast cancer.¹ Adverse events related to treatments have been extensively reported, including skeletal muscle deconditioning.^{2,3} Resulting from a global perturbation of muscle homeostasis, skeletal muscle deconditioning is characterized by both structural and functional alterations that will translate into a decrease in muscle mass and/or force as well as an increase in muscle fatigability.^{2,4,5} Skeletal muscle mitochondrial dysfunction and overall metabolic alterations represent another important aspect of skeletal muscle deconditioning,^{6–8} a maladaptation known to reduce the quality of life and contributing to an increased overall treatment-related toxicity that ultimately leads to a higher mortality risk.^{2,9–11}

Currently, mitochondrial alterations have been established as a frequent event related to muscle deconditioning in both pre-clinical^{12–14} and clinical settings.^{15–18} In breast cancer patients, a decrease in citrate synthase activity in the vastus lateralis muscle was observed in only one longitudinal study¹⁷ after chemotherapy exposure, reflecting a reduced mitochondrial content.¹⁹ When compared with healthy subjects, breast cancer patients also displayed a substantial reduction in mitochondrial content and size, both at intermyofibrillar and subsarcolemmal levels, at the end of CT treatment.¹⁶ Mitochondrial function also seemed directly impaired by chemotherapy. Indeed, two pre-clinical studies showed the potent negative impact of doxorubicin on mitochondrial respiratory capacity.^{12,20} As a consequence of mitochondrial dysfunction, fragmented and damaged mitochondria accumulate in skeletal muscle and, in addition to being less bioenergetically efficient, produce excessive amounts of reactive oxygen species (ROS). In pre-clinical models of doxorubicin administration in rodents, hydrogen peroxide (H₂O₂) production has been unanimously reported to be elevated.^{12,14} However, there is still no clinical study available in cancer patients to confirm this increased ROS production.

Mechanistically, previous studies highlighted altered mitochondrial dynamics, with decreased fusion and increased fission, leading to mitochondrial fragmentation, as observed in pre-clinical models,^{21,22} and in gastric cancer patients.²³ Mitochondrial remodelling by fission and fusion processes is essential for the removal of damaged mitochondria through mitophagy. In breast cancer patients, a decrease in PINK1 protein expression with no variation in Parkin protein levels was found,¹⁷ suggesting that mitophagy was likely down-regulated or unchanged. However, if this study provided interesting insights through indirect evidence,¹⁷ no study directly investigated alterations in mitochondrial dynamics in breast cancer (neither pre-clinical nor clinical models). Another mechanism potentially explaining the decrease in mitochondrial content is a reduction in mitochondrial biogenesis. Indeed, RNAseq

analysis performed on breast cancer patients^{15,18} showed a clear dysregulation of multiple genes implicated in overall mitochondrial homeostasis, including a reduction in PGC-1 α , the master regulator of mitochondrial biogenesis.

In this context, skeletal muscle mitochondrial alterations appear to represent a major event implicated in muscle deconditioning and may explain the high prevalence of cardiorespiratory deconditioning classically observed in patients treated for early breast cancer.² However, very few clinical studies have been conducted to explore the underlying mechanisms. Therefore, this study was dedicated to investigating overall skeletal muscle mitochondrial homeostasis in early breast cancer patients treated by CT, including mitochondrial quantity, function, and dynamics.

Material and methods

Participants and study design

Patients from the Institut de Cancérologie Strasbourg Europe (ICANS) were included in the PROTECT-03 study (NCT04638712). All participants provided written informed consent prior to enrolment, and the study was conducted in accordance with both the Declaration of Helsinki and the ethics approval received from the national ethics committee (2020-A01266-33). The participants performed two visits, including a muscle biopsy procedure: before the first CT administration (pre-CT) and within 1 week after the last CT administration (post-CT).

The eligibility criteria included non-pregnant women of at least 18 years old with a World Health Organization performance status of 0–2 who were diagnosed with breast cancer treated by anthracycline-cyclophosphamide and taxane-based (neo)adjuvant CT. Women were excluded if they had psychiatric, musculoskeletal, or neurological disorders and if they had already received chemotherapeutic agents. All patients received steroids the day of anthracycline administration and the two following days to prevent nausea and vomiting. The patients did not receive nutritional support or anabolic therapy.

Skeletal muscle biopsies

Skeletal muscle biopsy was obtained from the left *vastus lateralis* muscle and performed at 62.5% between the anterior superior iliac spine and the lateral condyle of the femur, according to a well-established method²⁴ using a 5 mm Bergström biopsy needle under sterile conditions and local anaesthesia (1% lidocaine). Pre-CT and post-CT biopsies were obtained from the same leg and at the same time in the morning. Patients were asked not to practice rigorous exercise at least 24 h prior to each visit. They were also asked

to eat the same breakfast for the two visits while sources of proteins, caffeine, and theine were prohibited. Tissue for mitochondrial respiration, H_2O_2 , and superoxide anion production measurements was immediately immersed in Krebs HEPES Buffer, and tissue for western blotting analysis was immediately frozen in liquid nitrogen and stored at -80°C .

Mitochondrial respiratory capacity recording

Within 1 h post-biopsy intervention, muscle was dissected, and muscle fibres were permeabilized by incubation under stirring for 30 min at 4°C in buffer S (CaK₂EGTA 2.77 mM, K₂EGTA 7.23 mM, Na₂ATP 6.04 mM, MgCl₂ 6.56 mM, taurine 20 mM, Na₂ Phosphocreatine 12.3 mM, imidazole 20 mM, dithiothreitol 0.5 mM, K-methane sulfonate 50 mM, pH 7.0 at 4°C) with saponin (50 $\mu\text{g}/\text{mL}$). Then, muscle fibres were incubated under stirring for 10 min at 4°C in buffer S without saponin. Mitochondrial oxygen respiratory capacity was analysed using a Clark electrode in a thermostated oxygraphic chamber at 37°C with continuous stirring (Oxygraph-2k, Oroboros instruments, Innsbruck, Austria). Briefly, fibres (2–3 mg wet weight) were placed in 2 mL of buffer in an oxygraphic chamber. Then, basal oxygen consumption of the complex I (CI)-linked substrate state due to proton leakage in the presence of glutamate (10 mM) and malate (2.5 mM) was measured. Oxidative phosphorylation (OXPHOS) by CI was recorded after the addition of saturating amounts of ADP (2 mM), OXPHOS by CI&CII after the addition of succinate (25 mM), and OXPHOS by CII after the addition of rotenone (0.5 μM). Data analysis was performed in duplicate using Oxygraph-2k-DatLab software version 6.2, and results are expressed in pmol/s/mg wet weight.

H_2O_2 measurement

H_2O_2 production in saponin-skinned muscle fibres was determined with 20 μM Amplex Red (Sigma), which reacts with H_2O_2 in a 1:1 stoichiometry catalysed by horseradish peroxidase (HRP; 1 U/mL, Sigma) to yield the fluorescent compound resorufin and a molar equivalent of H_2O_2 . Fluorescence was measured simultaneously with mitochondrial respiratory capacity recording on the high-resolution oxygraph. Thus, Amplex Red (20 μM) and HRP (1 U/mL) were added to the Oroboros chambers at the beginning of the experiment. The results are expressed in pmol/s/mg wet weight.

Superoxide anion measurement

Electron paramagnetic resonance (EPR) was performed to determine the production of superoxide anions using the specific spin probe 1-hydroxy-3-methoxycarbonyl-2,2,5,5-tetramethylpyrrolidine hydrochloride (CMH). Minced muscle

samples were washed twice with Krebs HEPES Buffer containing 25 μM deferoxamine and 5 $\mu\text{mol}/\text{L}$ diethyldithiocarbamate (DETC) to minimize CMH auto-oxidation. Then, samples were incubated in a plate at 37°C with CMH (200 μM) for 30 min under 20 mmHg oxygen partial pressure (mimicking physiological conditions) using a gas controller (Noxygen Sciences Transfer). Supernatant (40 μL) was injected in a disposable capillary tube and placed in an E-SCAN benchtop EPR spectrometer (Bruker-Biopsin, Rheinstetten, Germany) at 15°C . Detection of ROS unpaired electrons was conducted under the following EPR settings: centre field 3461.144 G, microwave power 21.85 mW, modulation amplitude 2.40 G, sweep time 5.24 s (10 scans), sweep width 60 G, and number of lag curve points 1. Tissues were finally dried at 150°C for 15 min. Superoxide anion production analysis were performed in duplicate using Bruker BioSpin WinEPR Spectrometer Software version 4.5, and results are expressed in $\mu\text{mol}/\text{min}/\text{mg}$ dry weight.

Western blotting and antibodies

Muscle samples were homogenized in 10 volumes of lysis buffer [50 mM Tris-HCl (pH 7.5), 150 mM NaCl, 1 mM egtazic acid, 1 mM EDTA, 100 mM NaF, 5 mM Na₃VO₄, 1% Triton X-100, 1% sodium dodecyl sulfate (SDS), 40 mM β -glycerophosphate, and protease inhibitor mixture (P8340; Sigma-Aldrich)] and centrifuged at 10 000g for 10 min (4°C), as in the studies of Pagano *et al.*²⁵ and Arc-Chagnaud *et al.*²⁶ Forty micrograms of protein extracts was loaded into 5–15% SDS-polyacrylamide gels and transferred onto nitrocellulose or PVDF membranes (iBlot 2 Dry Blotting System, Invitrogen). The membranes were blocked for 1 h at room temperature with 50 mM Tris-HCl (pH 7.5), 150 mM NaCl, and 0.1% Tween 20 (TBS-T) containing 5% skimmed milk. The membranes were incubated overnight at 4°C with the following primary antibodies: anti-4-HNE (Abcam, AB46545, 1:4000), anti-Bax (Santa Cruz, Sc-7480, 1:100), anti-Bcl-2 (Santa Cruz, Sc-7382, 1:200), anti-catalase (Genetex, GTX110704, 1:1000), anti-citrate synthase (Santa Cruz, Sc-390693, 1:200), anti-caspase 3 (Thermo Fisher Scientific, MA1-91637, 1:500), anti-COX IV (Santa Cruz, Sc-376731, 1:200), anti-p-DRP1 (Ser616, Cell Signalling, #34555, 1:1000), anti-DRP1 (Cell Signalling, #5391S, 1:1000), anti-p-eiF2 α (Ser 51, Cell Signalling, #9722S, 1:1000), anti-eiF2 α (Cell Signalling, #3398S, 1:1000), anti GPx1 (Thermo Fisher Scientific, PA5-26323, 1:1000), anti-Fis1 (Santa Cruz, Sc-376447, 1:200), anti-MNF1 (Thermo Fisher Scientific, PA5-38042, 1:1000), anti-MFN2 (Santa Cruz, Sc-100,560, 1:200), anti-Mul1 (Abcam, AB209263, 1:1000), anti-p-p38 MAPK (Thr180/Tyr182, Cell Signalling, #9211, 1:1000), anti-OPA1 (Thermo Fisher Scientific, MA5-16149, 1:1000) anti-p38 MAPK (Cell Signalling, #9212 1:1000), anti-p-p53 (Ser15, Cell Signalling, #9286S, 1:1000), anti-p53 (Cell Signalling, #2524S, 1:1000), anti-Parkin (Abcam, AB77924, 1:2000),

anti-PINK1 (Thermo Fisher Scientific, PA1-16604, 1:500), PGC-1 α 1 (Millipore, AB3242, 1:1000), anti-SOD2 (Genetex, GTX116093, 1:1000), and anti-VDAC (Santa Cruz, Sc-390996, 1:200). Then, the membranes were washed three times with TBS-T and incubated with anti-rabbit (Cell Signalling, 1:4000 #7074S) or anti-mouse (Cell Signalling, 1:4000 #7076S) secondary antibodies at room temperature for 1 h. The blots were revealed using a Pierce ECL kit (Thermo Fisher Scientific) or SupraSignal Femto kit (Thermo Fisher Scientific), and proteins were visualized by enhanced chemiluminescence (iBright 1500 Imaging System, Invitrogen) and quantified with the ImageJ Software (version 1.8.0). Ponceau coloration was used as the loading control.

Carbonylated protein determination

As described by Arc-Chagnaud *et al.*,²⁶ we determined carbonylated protein levels through immunoblot detection using an 'OxyBlot' protein oxidation kit (Millipore, MA, USA) according to the manufacturer's instructions. Total protein carbonyls were visualized by enhanced chemiluminescence (iBright 1500 Imaging System, Invitrogen) and quantified with the ImageJ software (version 1.8.0). Ponceau coloration was used as the loading control.

Sample size calculation and statistical analysis

Based on the study of Mijwel *et al.*¹⁷ showing a 30% (\pm 30%) decrease in mitochondrial content (through indirect measurement) in breast cancer patients after chemotherapy treatment, we predicted a similar decrease in our study. We chose VDAC protein levels as marker of mitochondrial content^{27,28} and calculated our sample size with an effect size of 1.2, an α risk of 0.05 and a 1- β risk of 0.95. We found a to-

tal of 10 patients to include, and considering a 30% dropout, we finally enrolled 13 patients.

The Shapiro–Wilk test was used to check the data normality. Appropriate parametric or non-parametric analyses were then performed (*t*-test or Wilcoxon tests, respectively) to compare pre-CT and post-CT variables. Statistical significance was set at $P < 0.05$, and all values are expressed as the mean \pm standard deviation (SD). Statistical analyses and graphs were made with the GraphPad Prism 6 software.

Results

Patient characteristics

A total of 25 patients were screened, and 13 patients were included in the study (Figure 1). Participants' characteristics are shown in Table 1. Two patients were unwilling to undergo the second muscle biopsy, and they were excluded from the analysis. No adverse events of special interest occurred over chemotherapy. No clinical adverse events were reported following the investigational biopsy process. All samples were assessable for biological tests as scheduled. Pre-CT, the time-point for biopsy collection was 5 ± 6 days (all biopsies were performed before the first CT administration). Post-CT, namely, after 18 ± 1 weeks of treatment by CT, the time-point collection was 7 ± 3 days.

Mitochondrial loss and reduced biogenesis

We found an important decrease in key markers of mitochondrial quantity, reaching -52% for citrate synthase protein levels ($P = 0.02$; Figure 2A) and -38% for VDAC protein levels ($P = 0.04$; Figure 2B). We therefore measured PGC-1 α 1 protein levels and found a reduction in its protein expression (-29.5% ; $P = 0.04$; Figure 2C).

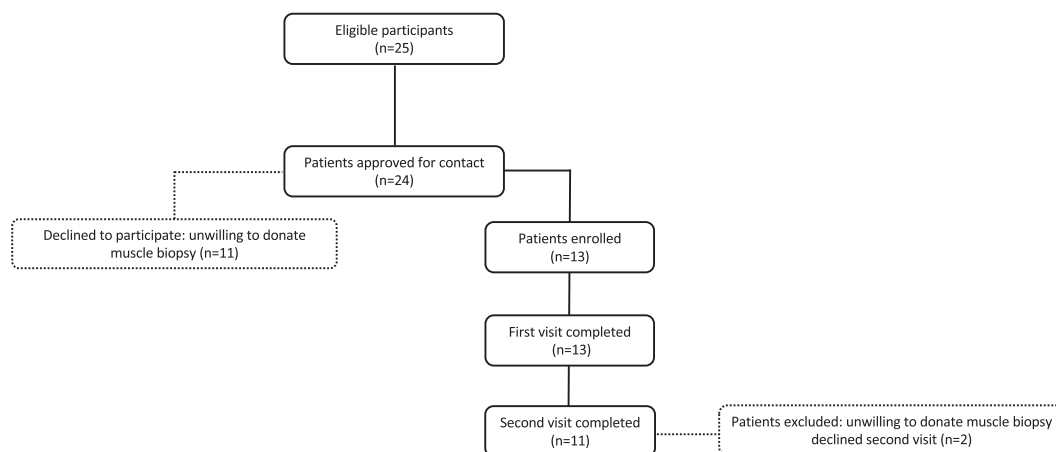


Figure 1 Flow chart of the participants.

Table 1 Participants characteristics

Participants characteristics	n = 11
Characteristic (mean ± SD)	
Age (year)	56 ± 12
Body mass pre-CT (kg)	75 ± 16
Body mass post-CT (kg)	74 ± 15
Body mass index pre-CT (kg/m ²)	29 ± 7
Body mass index post-CT (kg/m ²)	29 ± 6
WHO performance status pre-CT (n)	
0	9
1	2
WHO performance status post-CT (n)	
0	9
1	2
Tumour SBR grade (n)	
I	1
II	4
III	6
Tumour stage (n)	
1	2
2	4
3	5
Tumour type (n)	
Triple negative	3
Luminal (A/B)	5
HER2-positive	3
Treatment setting (n)	
Adjuvant	6
Neo-adjuvant	5
Chemotherapy regimen (n)	
Anthracycline-cyclophosphamide followed by paclitaxel	8
Anthracycline-cyclophosphamide followed by paclitaxel + trastuzumab	3

CT, chemotherapy; HER2, human epidermal growth factor receptor 2; SBR, Scarff-Bloom-Richardson; WHO, World Health Organization performance status.

Mitochondrial dynamics and mitophagy

Mitochondrial dynamics were impaired, as showed by an important decrease in MFN2 protein expression (−33.4%; $P = 0.01$; Figure 3A), a key marker of mitochondrial outer membrane fusion, while MFN1 protein levels were unchanged ($P = 0.1$ and $P = 0.6$ for the 85 and 71 kDa isoforms, respectively, Figure 3B). Regarding OPA1, a marker of mitochondrial inner membrane fusion, we detected the long form (L-OPA1) and three short isoforms (S1, S2, and S3).²⁹ We only found a decrease in S3-OPA1 (−32.8%; $P = 0.04$) while the other isoforms remained stable ($P > 0.05$; Figure 3C). The mitochondrial fission process, investigated through Fis1 ($P = 0.9$; Figure 3D) and DRP1 ($P = 0.9$; Figure 3E) protein levels, remained unchanged. We also did not find any variations in Parkin ($P = 0.2$; Figure 3F) or PINK1 ($P = 0.3$; Figure 3G) protein levels, both essential proteins of the mitophagy process. Mul1, a mitochondrial E3 ubiquitin protein ligase implicated in the initiation of mitophagy, remained stable ($P = 0.6$; Figure 3H), emphasizing that mitophagy seemed to be unchanged in pre-CT vs. post-CT. However, we found an increase in mitophagic potential, reflected by the ratio of Parkin/VDAC (+176.4%; $P = 0.02$; Figure 3I) protein levels.³⁰

Mitochondrial respiration and reactive oxygen species production

We found no variation in the mitochondrial respiratory capacity for all complexes investigated between pre-CT and post-CT ($P > 0.05$ for all substrate additions; Figure 4A and

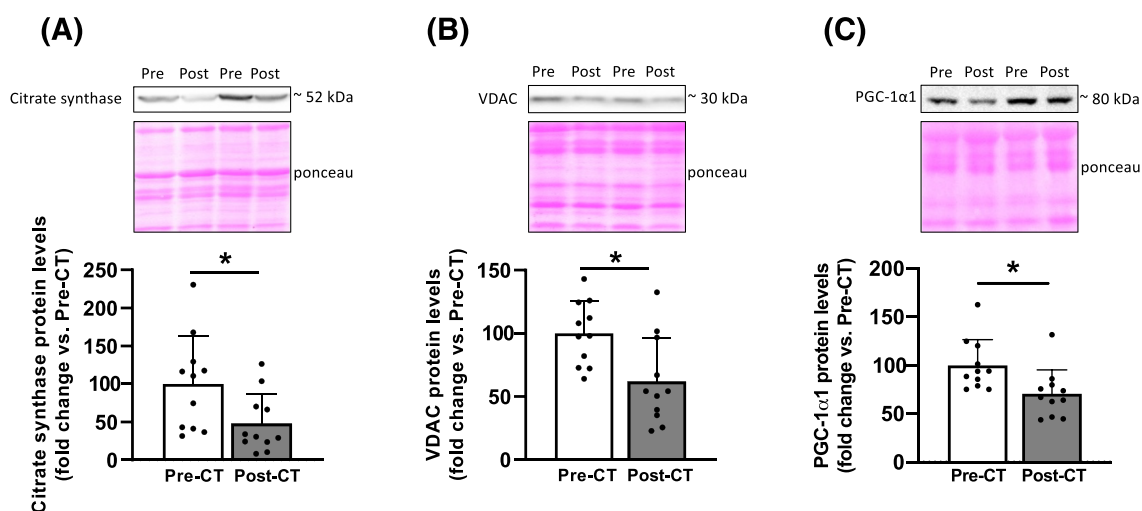


Figure 2 Changes in key markers of mitochondrial quantity and mitochondrial biogenesis. Citrate synthase (A), VDAC (B), and PGC-1α1 (C) protein levels from vastus lateralis muscle biopsies taken before (pre-CT) and after (post-CT) breast cancer chemotherapy (CT). Above each panel, western blots from two representative subjects are displayed. All values are expressed as the mean ± SD ($N = 11$). * $P < 0.05$.

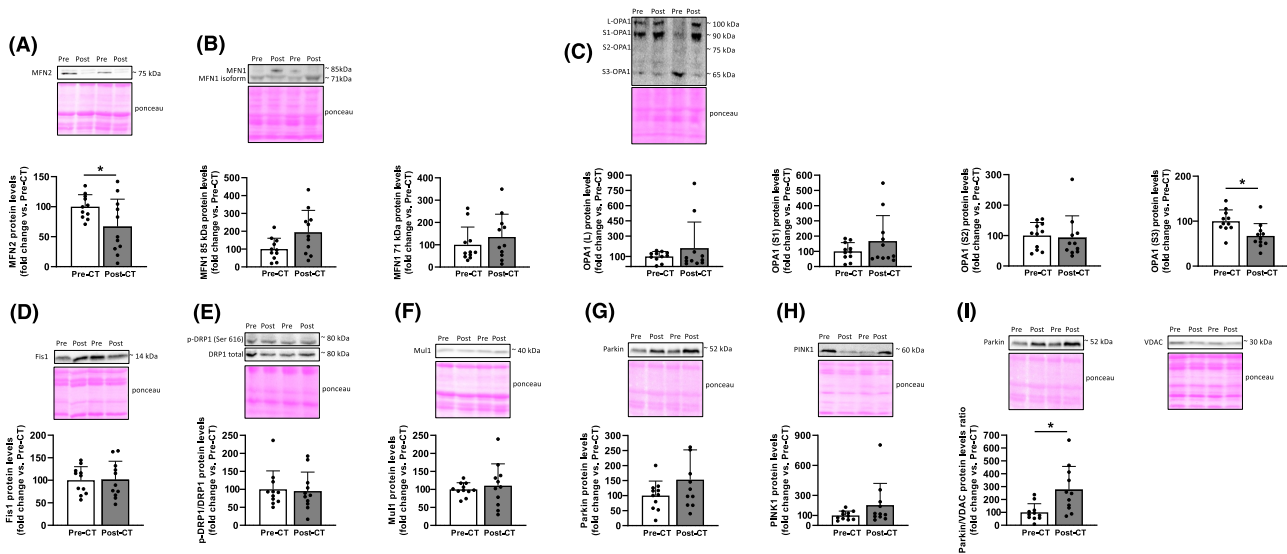


Figure 3 Changes in protein markers of mitochondrial dynamics and mitophagy. MFN2 (A); MFN1 85 and 71 kDa isoforms (B); OPA1 isoforms: L, S1, S2, and S3 (C); Fis1 (D); p-DRP1 (Ser616)/DRP1 (E); Mu1 (F); Parkin (G); PINK1 (H); and Parkin/VDAC (I) protein levels from vastus lateralis muscle biopsies taken before (pre) and after (post) breast cancer chemotherapy (CT). Above each panel, western blots from two representative subjects are displayed. All values are expressed as the mean \pm SD ($N = 11$). * $P < 0.05$.

4B), demonstrating that O_2 consumption was not altered by CT. Similarly, we did not observe any variation in COX IV protein levels (Figure 4C). Importantly, we found a significant elevation in H_2O_2 produced at all stages of the experiment between pre-CT and post-CT (Figure 4D and 4E), with increases in H_2O_2 levels for the CI-linked substrate state (+26.8%; $P = 0.001$), OXPHOS by CI (+16.7%; $P = 0.009$), CI&CII (+23.9%; $P = 0.002$), and CII (+21.8%; $P = 0.02$). We also reported a 21% decrease in superoxide anion production ($P = 0.02$; Figure 4F), which is consistent with the H_2O_2 produced due to superoxide anion dismutation. Despite an increase in H_2O_2 production, we observed no significant change in the lipid peroxidation marker 4-HNE ($P = 0.18$; Figure 4G) or in the total carbonylated protein levels ($P = 0.68$; Figure 4H). Interestingly, the protein levels of the antioxidant enzymes SOD2 ($P = 0.8$; Figure 4I), catalase ($P = 0.4$; Figure 4J), and GPx1 ($P = 0.7$; Figure 4K) were also unchanged between pre-CT and post-CT. Additionally, H_2O_2 downstream signalling was not upregulated post-CT, as evidenced by eIF2 α ($P = 0.30$, Figure 4L), p38 MAPK ($P = 0.63$, Figure 4M), and p53 ($P = 0.21$, Figure 4N).

Induction of the apoptosis process

We investigated apoptosis, the programmed cell death process, which is mainly regulated by mitochondria.³¹ An increase in the protein levels of the proapoptotic marker Bax was found (+72.0%; $P = 0.04$; Figure 5A), whereas the protein levels of the antiapoptotic marker Bcl-2 remained stable ($P = 0.3$; Figure 5B) between pre-CT and post-CT. However,

the increased active (cleaved)-caspase 3/pro-caspase 3 ratio did not reach significance (+68.8%; $P = 0.1$; Figure 5C).

Discussion

The aim of this study was to identify the cellular mechanisms involved in skeletal muscle mitochondrial homeostasis alterations in patients treated for early breast cancer through (neo)adjuvant chemotherapy. Chemotherapy treatment definitively reduced mitochondrial content and biogenesis, impaired mitochondrial dynamics and mitophagy, increased H_2O_2 production, as well as initiated apoptosis as a response to global mitochondrial homeostasis disruption (Figure 6).

Reduced mitochondrial content and biogenesis

We first confirmed that early breast cancer patients undergoing chemotherapy significantly lost mitochondria. Indeed, we found a substantial decrease in both citrate synthase and VDAC protein levels, two key markers of mitochondrial quantity.^{26,28,32} These results confirmed previous investigations showing reduced mitochondrial content in breast cancer patients at the end of their treatment compared with healthy matched controls¹⁶ and a decrease in citrate synthase activity in patients during CT.¹⁷ This mitochondrial loss appears to be a strong maladaptation consecutive to breast cancer and its treatment. Importantly, mitochondrial biogenesis (investigated through PGC-1 α protein levels) was only investigated, to date, in pre-clinical models.^{21,22,28,33} In this clinical study, we documented a significant decrease in PGC-1 α pro-

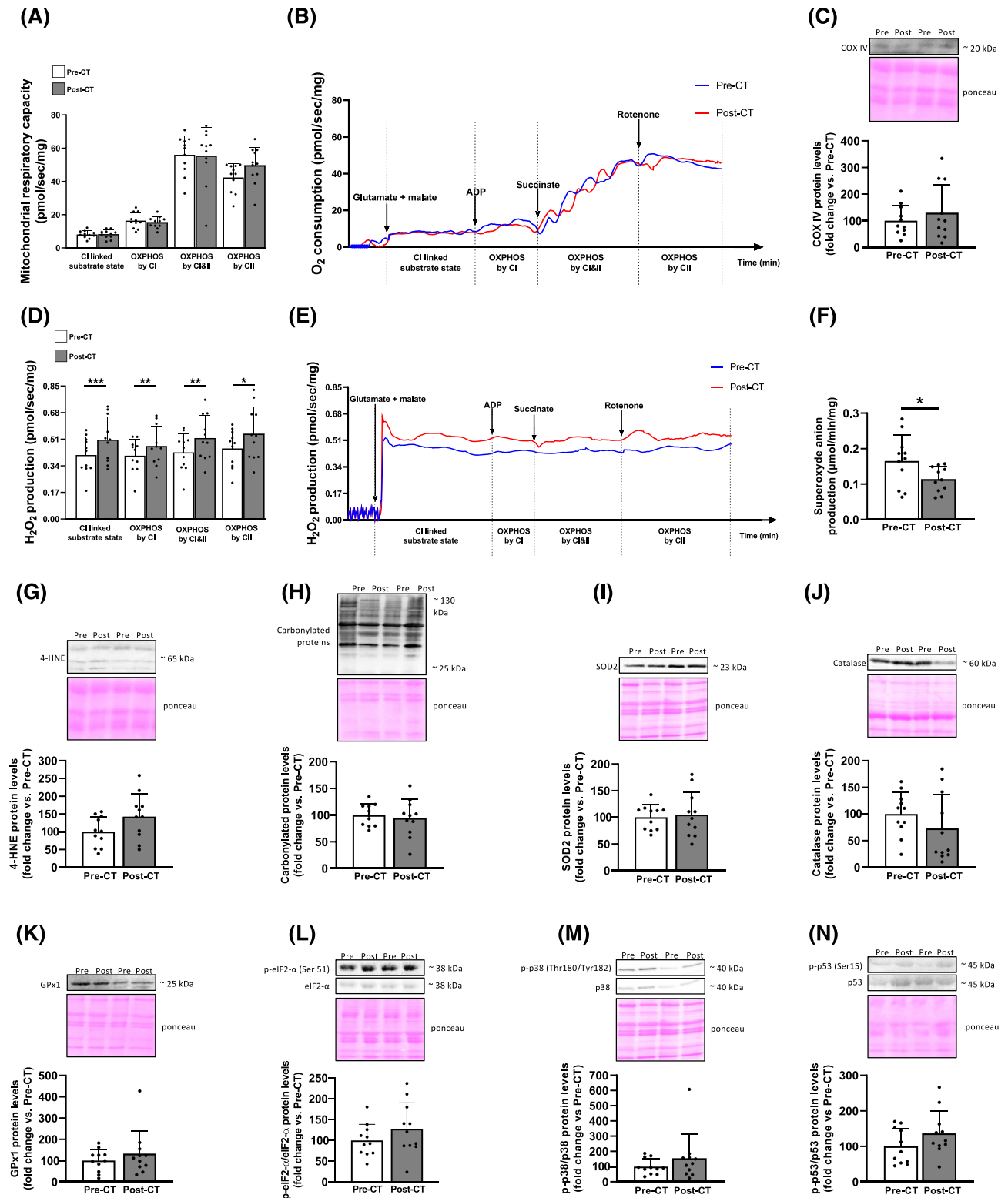


Figure 4 Changes in mitochondrial respiration, reactive oxygen species production, and redox signalling protein markers. Mitochondrial respiratory capacity quantification (A), and associated mean representative curves (B), for CI-linked substrate state, OXPHOS by CI, OXPHOS by CI&CII, and OXPHOS by CII on permeabilized fibres from vastus lateralis muscle biopsies taken before (pre) and after (post) breast cancer chemotherapy (CT). COX IV (C) protein levels in pre-CT vs. post-CT. H₂O₂ production quantification (D), and associated mean representative curves (E), for CI-linked substrate state, OXPHOS by CI, OXPHOS by CI&CII, and OXPHOS by CII in pre-CT vs. post-CT permeabilized fibres. Superoxide anion measurement (F) through electron paramagnetic resonance in pre-CT vs. post-CT minced muscle samples. 4-HNE (G), total carbonylated (H), SOD2 (I), catalase (J), GPx1 (K), p-eIF2 α (Ser51)/eIF2 α (L), p-p38 MAPK (Thr180/Tyr182)/p38 MAPK (M) and p-p53 (Ser15)/p53 (N) protein levels in pre-CT vs. post-CT. Above each panel with western blot analyses, two representative subjects are displayed. All values are expressed as the mean \pm SD (N = 11). *P < 0.05; **P < 0.01; ***P < 0.001; CI: complex I; CII: complex II; OXPHOS: oxidative phosphorylation.

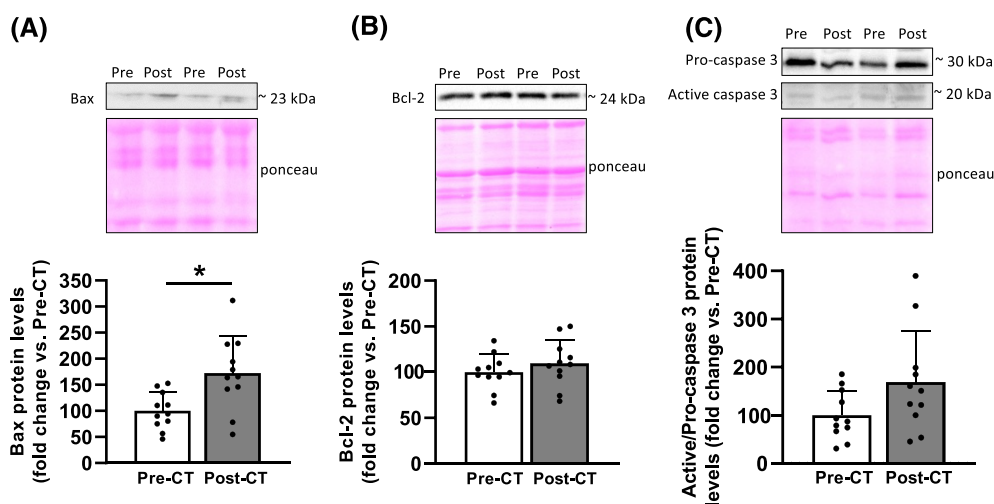


Figure 5 Changes in protein markers of apoptosis induction. Bax (A), Bcl-2 (B), and active/pro-caspase 3 (C) protein levels from vastus lateralis muscle biopsies taken before (pre) and after (post) breast cancer chemotherapy (CT). Above each panel, western blots from two representative subjects are displayed. All values are expressed as the mean \pm SD (N = 11). *P < 0.05.

tein levels, suggesting that the chemotherapy-induced loss of mitochondria is explained, at least in part, by a reduction in mitochondrial biogenesis.

Impaired mitochondrial dynamics and the mitophagy paradox

The processes of mitochondrial fusion and fission form a delicate balance that results in highly dynamic structures.⁷ In the present study, we did not report any change in two different fission markers (Fis1 and DRP1). However, we found a significant decrease in the mitochondrial fusion marker MFN2 without any change in MFN1 protein levels, documenting a dysregulation in the outer-membrane fusion process balance. If L-OPA1 protein levels were unchanged, suggesting that inner membranes fusion was preserved,³⁴ the coordination between outer and inner membranes fusion is needed to result in healthy mitochondria³⁵ and, altogether, our results suggest that the fusion process was impaired post-CT. Only documented in pre-clinical models of other cancers^{21,22} and in gastric cancer patients,²³ this impaired fusion process may indicate an overall altered mitochondrial

dynamics, leading to fragmented mitochondria.^{21,33} This postulate is further supported by the reduction found in S3-OPA1 protein levels, which has been previously reported to cause mitochondrial fragmentation.³⁶ Mitophagy represents an essential process to remove fragmented and damaged mitochondria, and we found no change in the protein levels of different key markers (Parkin, PINK1, and Mul1). Consequently, two contradictory hypotheses can be suggested: defective mitophagy or a relative increase in mitophagy. The first hypothesis, most likely intuitive, is that the mitophagy process is defective in breast cancer patients undergoing CT. Indeed, the altered mitochondrial dynamics and the presumably increased number of damaged mitochondria should have led to the activation of the mitophagy process to remove these dysfunctional mitochondria. This hypothesis is strengthened by studies emphasizing that mitophagy is dysfunctional in cancer cachexia through a decrease in PINK1 or Parkin levels.^{12,17,23,37} In contrast, the second hypothesis is based on an increase in the relative activity of the mitophagy process. While we and others^{16,17} found a substantial decrease in mitochondrial content, the same amount of mitophagy should result in an increased mitophagic potential, reflected by the ratio between Parkin

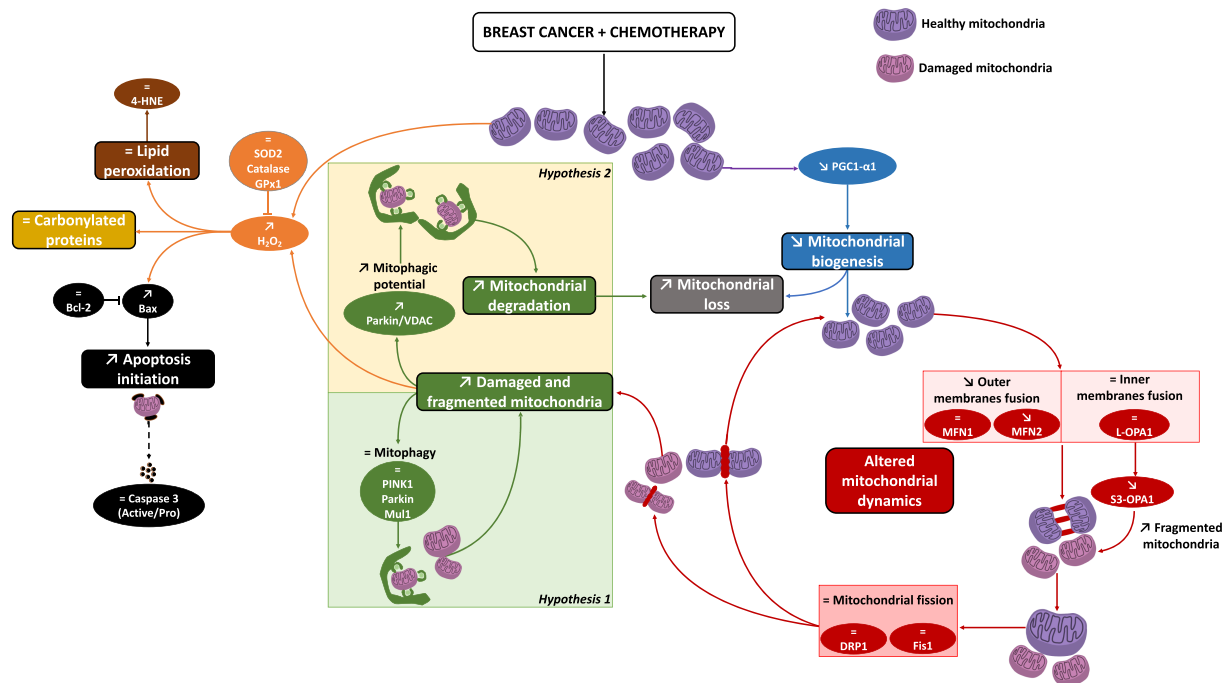


Figure 6 Summary of the mitochondrial alterations observed in early breast cancer patients undergoing chemotherapy. Through the analysis of vastus lateralis muscle biopsies taken before (pre) and after (post) breast cancer chemotherapy (CT), we identified an increased mitochondrial loss (grey box) that may be explained by a decrease in PGC-1 α 1 protein levels, reflecting a reduced mitochondrial biogenesis process (in blue). Mitochondrial dynamics (in red) were also impaired, as evidenced by a dysregulation in the fusion process, mediated by a decrease in the mitochondrial outer membrane fusion marker MFN2, without any change in MFN1 and OPA1. No change was observed in fission markers (Fis1 and DRP1), indicating a dysregulation in the mitochondrial fusion/fission balance. These alterations are likely leading to the accumulation of fragmented and damaged mitochondria (rose-coloured mitochondria), corroborated by the accumulation of S3-OPA1 isoform. As a consequence, fragmented and damaged mitochondria accumulate in skeletal muscle and produce excessive amounts of reactive oxygen species such as H₂O₂ (in orange). As mentioned above, we found no change in mitochondrial fission, a prerequisite step for the activation of mitophagy. Despite the absence of change in the expression of different mitophagy markers (Parkin, PINK1, and Mu11; in green), two contradictory hypotheses arise from these results: defective mitophagy (Hypothesis 1) or a relative increase in mitophagy (increased mitophagic potential reflected by the Parkin/VDAC ratio; Hypothesis 2). Antioxidant enzyme (in orange), lipid peroxidation (in brown), and carbonylated protein levels (in yellow) were unchanged. However, we found a large increase in Bax protein levels, a proapoptotic protein that initiates apoptosis, and no change was observed for Bcl-2, its antiapoptotic counterpart (in black). While several pre-clinical studies found increased levels in the active (cleaved)-caspase 3/pro-caspase 3 ratio, the slight increase observed in our study did not reach significance (in black dotted line).

and VDAC protein levels.^{12,30,38} This ratio was dramatically increased in our study, suggesting a relative increase in mitophagy per mitochondrion. However, this ratio alone is only indicative and the localization of Parkin should be determined, considering that cytosolic p53 can sequester Parkin and disturbs its translocation, leading to a reduced mitophagy, and promoting the accumulation of damaged mitochondria.^{39,40} These two hypotheses contradict each other and reflect the need to better understand mitochondrial dynamics and mitophagy in breast cancer patients.

Unchanged mitochondrial respiratory capacity and increased reactive oxygen species production

Since we found an alteration in mitochondrial content, biogenesis, and dynamics, we next investigated mitochondrial func-

tion and ROS production. We first measured COX IV protein levels, an essential protein implicated in the electron transport chain, and found no variation in its expression. We then explored mitochondrial respiratory capacity and also found no change from pre- to post-CT. While mitochondrial function seems to be preserved, we found an increase in H₂O₂ production levels and expanded, in cancer patients, previous results obtained in pre-clinical models after CT administration.^{22,41,42} Although excessive ROS production is classically associated with impaired mitochondrial respiratory capacity,⁷ a significant increase in H₂O₂ without any change in mitochondrial respiratory capacity at 4 weeks of anthracycline-based CT treatment was previously shown in mice.¹² In the same study, a decrease in mitochondrial respiratory capacity was observed 12 weeks after the last CT administration, highlighting that CT may induce a long-term, and not a short-term, impairment of skeletal muscle mitochondrial respiration. Therefore, by extrapolating

these results from mice to patients, the reduction in mitochondrial respiratory capacity might not develop immediately but would rather appear in the following weeks after CT completion. Further studies are needed to confirm this hypothesis and explore the extent of the severity and duration of mitochondrial dysfunction after CT.

In addition to excessive H₂O₂ production, a decrease in superoxide anion levels was observed. This could be explained by the dismutation of superoxide anion in the presence of SOD2, an important ROS scavenger. While Mijwel *et al.*¹⁷ observed an increase in SOD2 protein expression after CT, we did not find any variation in our study. This discrepancy may be explained by the later time point of post-CT biopsy collection in our study. Indeed, our post-CT measurement was performed ~7 days after the last CT to prevent any acute effect of CT, whereas Mijwel *et al.*¹⁷ performed the post-CT biopsy 24 to 72 h after CT. Together with the fact that we cannot exclude an increase in SOD2 enzymatic activity without any change in its protein levels, the biopsy time-point collection may explain the difference found in SOD2 protein levels. This may provide a reason for the absence of variation in key H₂O₂ downstream signalling pathways (eIF2 α , p38 MAPK, and p53). Indeed, these proteins were likely up-regulated and/or phosphorylated acutely after CT, as demonstrated in rodent studies with CT administration.^{33,43}

Altered oxidative balance without oxidative damage: A matter of reactive oxygen species production intensity?

Mitochondria have been identified as the main ROS generators in muscle cells,⁷ and considering the 'double-edged sword' nature of ROS, excessive levels of ROS production may induce oxidative stress and produce adverse modifications to cell components (DNA, proteins, and lipids). Under normal conditions, antioxidant defences and ROS counterbalance each other to maintain adequate oxidative balance and preserve cells against these oxidative damages. In this study, we then explored key antioxidant enzymes (catalase and GPx1) and found no increase in their protein expression. Therefore, there is an altered oxidative balance in breast cancer patients undergoing CT, potentially resulting in an increased oxidative stress. In this context, we investigated both lipid peroxidation marker 4-HNE and carbonylated protein levels and found no change from pre-CT to post-CT. These results strongly emphasize that this increase in ROS production, 7 days after CT completion, might not be intense enough to induce oxidative stress and produce oxidative damages to proteins and lipids. However, two pre-clinical studies demonstrated increased lipid peroxidation and carbonylated proteins levels 24 and 48 h after doxorubicin administration,^{44,45} showing that oxidative damage may occur in the early stages

after CT administration. Differences in ROS production intensity might represent an explanation to these discrepancies. Indeed, we found a 22% increase in H₂O₂ levels 7 days after the last CT administration while others showed larger increases (more than 100%) 2 and 24 h²⁰ as well as 48 h⁴⁵ after CT administration in rodents, indicating that ROS production intensity appears essential and might underlie the dose–response effect on oxidative stress damage. We therefore cannot exclude the possibility that breast cancer patients experienced substantial ROS production during their treatment, and consequently oxidative stress-related cellular damage, but further studies are needed in order to explore this hypothesis.

Increased apoptosis initiation as a response to global mitochondrial homeostasis disruption

We finally investigated the apoptosis pathway, a process mainly controlled by mitochondria,³¹ an organelle that we found to be substantially disrupted in breast cancer patients after CT. We found a significant increase in the protein levels of Bax, a proapoptotic protein that initiates apoptosis, and no change in Bcl-2, its antiapoptotic counterpart. Surprisingly, the initiation of apoptosis was not associated with an increase in active/pro caspase 3 protein level ratio ($P = 0.1$), which did not fully support the idea of an overactivated apoptosis pathway in breast cancer patients undergoing CT. Considering that many pre-clinical studies documented an overactivated apoptosis pathway,² further studies are needed to explore apoptosis in breast cancer patients skeletal muscle.

Conclusions

This clinical study, conducted in early breast cancer patients undergoing chemotherapy, highlighted severe skeletal muscle alterations. Specifically, this study identified four major mitochondrial alterations: (i) a striking reduction in the mitochondrial biogenesis marker PGC-1 α 1, (ii) altered mitochondrial dynamics through weakened fusion process and potential mitophagy defects, (iii) exacerbated mitochondria-mediated H₂O₂ production, and (iv) an initiation of the apoptosis pathway. All of these alterations likely explain, at least in part, the high prevalence of cardiorespiratory deconditioning classically observed in breast cancer patients.² Therefore, the characterization of mitochondrial alterations may help researchers and clinicians identify appropriate therapeutic interventions to counteract skeletal muscle deconditioning.

Acknowledgements

We would like to thank Fabienne Goupilleau and Isabelle Georg for their help with mitochondrial respiration experiments. We also thank Thomas Brioché and Sophie Schubnel for their assistance in the investigation of carbonylated proteins. Many thanks to both the Oncobiology Platform (Laboratory of Biochemistry and Molecular Biology) and Pathology and Cytology Department of the University Hospital of Strasbourg for their help with biopsy conditioning and storage. We finally particularly acknowledge our patients for their participation. This work was supported by the Institut de Cancérologie Strasbourg Europe (ICANS) and has been published under the framework of the IdEx Unistra supported by investments in the future programme of the French government.

Conflict of interest

The authors declare that the research was conducted in the absence of any commercial or financial relationships that could be construed as a potential conflict of interest.

Ethical guidelines statement

The authors of this manuscript certify that they have complied with ethical guidelines for authorship and publishing in the *Journal of Cachexia, Sarcopenia and Muscle*.⁴⁶

References

- Denduluri N, Chavez-MacGregor M, Telli ML, Eisen A, Graff SL, Hassett MJ, et al. Selection of optimal adjuvant chemotherapy and targeted therapy for early breast cancer: ASCO clinical practice guideline focused update. *J Clin Oncol Off J Am Soc Clin Oncol* 2018;**36**:2433–2443.
- Mallard J, Hucteau E, Hureau TJ, Pagano AF. Skeletal muscle deconditioning in breast cancer patients undergoing chemotherapy: current knowledge and insights from other cancers. *Front Cell Dev Biol* 2021;**9**:2550.
- Martin A, Freyssen D. Phenotypic features of cancer cachexia-related loss of skeletal muscle mass and function: lessons from human and animal studies. *J Cachexia Sarcopenia Muscle* 2021;**12**:252–273.
- Brioché T, Pagano AF, Py G, Chopard A. Muscle wasting and aging: experimental models, fatty infiltrations, and prevention. *Mol Aspects Med* 2016;**50**:56–87.
- Chopard A, Hillock S, Jasmin BJ. Molecular events and signalling pathways involved in skeletal muscle disuse-induced atrophy and the impact of countermeasures. *J Cell Mol Med* 2009;**13**:3032–3050.
- Beltrà M, Pin F, Ballarò R, Costelli P, Penna F. Mitochondrial dysfunction in cancer cachexia: impact on muscle health and regeneration. *Cell* 2021;**10**:3150.
- Hyatt HW, Powers SK. Mitochondrial dysfunction is a common denominator linking skeletal muscle wasting due to disease, aging, and prolonged inactivity. *Antioxid Basel Switz* 2021;**10**:588.
- Kemp PR, Paul R, Hinken AC, Neil D, Russell A, Griffiths MJ. Metabolic profiling shows pre-existing mitochondrial dysfunction contributes to muscle loss in a model of ICU-acquired weakness. *J Cachexia Sarcopenia Muscle* 2020;**11**:1321–1335.
- Mallard J, Hucteau E, Schott R, Petit T, Demarchi M, Belletier C, et al. Evolution of physical status from diagnosis to the end of first-line treatment in breast, lung, and colorectal cancer patients: the PROTECT-01 cohort study protocol. *Front Oncol* 2020;**10**:1304. <https://doi.org/10.3389/fonc.2020.01304>
- Caan BJ, Cespedes Feliciano EM, Prado CM, Alexeeff S, Kroenke CH, Bradshaw P, et al. Association of muscle and adiposity measured by computed tomography with survival in patients with nonmetastatic breast cancer. *JAMA Oncol* 2018;**4**:798–804.
- Baracos VE, Martin L, Korc M, Guttridge DC, Fearon KCH. Cancer-associated cachexia. *Nat Rev Dis Primers* 2018;**4**:17105.
- Gouspillou G, Scheede-Bergdahl C, Spendiff S, Vuda M, Meehan B, Mlynarski H, et al. Anthracycline-containing chemotherapy causes long-term impairment of mitochondrial respiration and increased reactive oxygen species release in skeletal muscle. *Sci Rep* 2015;**5**:8717.
- Nissinen TA, Degerman J, Räsänen M, Poikonen AR, Koskinen S, Mervaala E, et al. Systemic blockade of ACVR2B ligands prevents chemotherapy-induced muscle wasting by restoring muscle protein synthesis without affecting oxidative capacity or atrogenes. *Sci Rep* 2016;**6**:32695.
- Hiensch AE, Bolam KA, Mijwel S, Jeneson JAL, Huitema ADR, Kranenburg O, et al. Doxorubicin-induced skeletal muscle atrophy: elucidating the underlying molecular pathways. *Acta Physiol (Oxf)* 2020;**229**:e13400.
- Bohlen J, McLaughlin SL, Hazard-Jenkins H, Infante AM, Montgomery C, Davis M, et al. Dysregulation of metabolic-associated pathways in muscle of breast cancer patients: preclinical evaluation of interleukin-15 targeting fatigue. *J Cachexia Sarcopenia Muscle* 2018;**9**:701–714.
- Guigni BA, Callahan DM, Tourville TW, Miller MS, Fiske B, Voigt T, et al. Skeletal muscle atrophy and dysfunction in breast cancer patients: role for chemotherapy-derived oxidant stress. *Am J Physiol Cell Physiol* 2018;**315**:C744–C756.
- Mijwel S, Cardinale DA, Norrbom J, Chapman M, Ivarsson N, Wengström Y, et al. Exercise training during chemotherapy preserves skeletal muscle fiber area, capillarization, and mitochondrial content in patients with breast cancer. *FASEB J* 2018;**32**:5495–5505.
- Wilson HE, Stanton DA, Rellick S, Geldenhuys W, Pistilli EE. Breast cancer-associated skeletal muscle mitochondrial dysfunction and lipid accumulation is reversed by PPARγ. *Am J Physiol Cell Physiol* 2021;**320**(4):C577–C590.
- Larsen S, Nielsen J, Hansen CN, Nielsen LB, Wibrand F, Stride N, et al. Biomarkers of mitochondrial content in skeletal muscle of healthy young human subjects. *J Physiol* 2012;**590**:3349–3360.
- Gilliam LAA, Fisher-Wellman KH, Lin C-T, Maples JM, Cathey BL, Neuffer PD. The anticancer agent doxorubicin disrupts mitochondrial energy metabolism and redox balance in skeletal muscle. *Free Radic Biol Med* 2013;**65**:988–996.
- Brown JL, Rosa-Caldwell ME, Lee DE, Blackwell TA, Brown LA, Perry RA, et al. Mitochondrial degeneration precedes the development of muscle atrophy in progression of cancer cachexia in tumour-bearing mice. *J Cachexia Sarcopenia Muscle* 2017;**8**:926–938.
- Pin F, Barreto R, Kitase Y, Mitra S, Erne CE, Novinger LJ, et al. Growth of ovarian cancer xenografts causes loss of muscle and bone mass: a new model for the study of cancer cachexia. *J Cachexia Sarcopenia Muscle* 2018;**9**:685–700.
- Marzetti E, Lorenzi M, Landi F, Picca A, Rosa F, Tanganelli F, et al. Altered mitochondrial quality control signaling in

- muscle of old gastric cancer patients with cachexia. *Exp Gerontol* 2017;**87**:92–99.
24. Bergstrom J. Percutaneous needle biopsy of skeletal muscle in physiological and clinical research. *Scand J Clin Lab Invest* 1975; **35**:609–616.
 25. Pagano AF, Brioché T, Arc-Chagnaud C, Demangel R, Chopard A, Py G. Short-term disuse promotes fatty acid infiltration into skeletal muscle. *J Cachexia Sarcopenia Muscle* 2018;**9**:335–347.
 26. Arc-Chagnaud C, Py G, Fovet T, Roumanille R, Demangel R, Pagano AF, et al. Evaluation of an antioxidant and anti-inflammatory cocktail against human hypoactivity-induced skeletal muscle deconditioning. *Front Physiol* 2020; **11**:71. <https://www.ncbi.nlm.nih.gov/pmc/articles/PMC7028694/>
 27. Jacob KJ, Sonjak V, Spendiff S, Hepple RT, Chevalier S, Perez A, et al. Mitochondrial content, but not function, is altered with a multimodal resistance training protocol and adequate protein intake in leucine-supplemented pre/frail women. *Front Nutr* 2021;**7**:619216.
 28. Huot JR, Pin F, Narasimhan A, Novinger LJ, Keith AS, Zimmers TA, et al. ACVR2B antagonism as a countermeasure to multi-organ perturbations in metastatic colorectal cancer cachexia. *J Cachexia Sarcopenia Muscle* 2020;**11**:1779–1798.
 29. Ju W-K, Lindsey JD, Angert M, Patel A, Weinreb RN. Glutamate receptor activation triggers OPA1 release and induces apoptotic cell death in ischemic rat retina. *Mol Vis* 2008;**14**:2629–2638.
 30. Geisler S, Holmström KM, Skujat D, Fiesel FC, Rothfuss OC, Kahle PJ, et al. PINK1/Parkin-mediated mitophagy is dependent on VDAC1 and p62/SQSTM1. *Nat Cell Biol* 2010;**12**:119–131.
 31. Estaquier J, Vallette F, Vayssiere J-L, Mignotte B. The mitochondrial pathways of apoptosis. *Adv Exp Med Biol* 2012;**942**: 157–183.
 32. Shang H, Xia Z, Bai S, Zhang HE, Gu B, Wang R. Downhill running acutely elicits mitophagy in rat soleus muscle. *Med Sci Sports Exerc* 2019;**51**:1396–1403.
 33. Barreto R, Waning DL, Gao H, Liu Y, Zimmers TA, Bonetto A. Chemotherapy-related cachexia is associated with mitochondrial depletion and the activation of ERK1/2 and p38 MAPKs. *Oncotarget* 2016;**7**:43442–43460.
 34. Lee H, Yoon Y. Mitochondrial fission and fusion. *Biochem Soc Trans* 2016;**44**:1725–1735.
 35. Pernas L, Scorrano L. Mito-morphosis: mitochondrial fusion, fission, and cristae remodeling as key mediators of cellular function. *Annu Rev Physiol* 2016;**78**:505–531.
 36. Wang R, Mishra P, Garbis SD, Moradian A, Sweredoski MJ, Chan DC. Identification of new OPA1 cleavage site reveals that short isoforms regulate mitochondrial fusion. *Mol Biol Cell* 2021;**32**:157–168.
 37. Aversa Z, Pin F, Lucia S, Penna F, Verzaro R, Fazi M, et al. Autophagy is induced in the skeletal muscle of cachectic cancer patients. *Sci Rep* 2016;**6**:30340.
 38. Gouspillou G, Sgarioto N, Kapchinsky S, Purves-Smith F, Norris B, Pion CH, et al. Increased sensitivity to mitochondrial permeability transition and myonuclear translocation of endonuclease G in atrophied muscle of physically active older humans. *FASEB J* 2014;**28**:1621–1633.
 39. Koleini N, Kardami E. Autophagy and mitophagy in the context of doxorubicin-induced cardiotoxicity. *Oncotarget* 2017;**8**: 46663–46680.
 40. Hoshino A, Mita Y, Okawa Y, Ariyoshi M, Iwai-Kanai E, Ueyama T, et al. Cytosolic p53 inhibits Parkin-mediated mitophagy and promotes mitochondrial dysfunction in the mouse heart. *Nat Commun* 2013;**4**:2308.
 41. Chacon-Cabrera A, Mateu-Jimenez M, Langohr K, Femoselle C, García-Arumí E, Andreu AL, et al. Role of PARP activity in lung cancer-induced cachexia: effects on muscle oxidative stress, proteolysis, anabolic markers, and phenotype. *J Cell Physiol* 2017;**232**:3744–3761.
 42. Puig-Vilanova E, Rodriguez DA, Lloreta J, Ausin P, Pascual-Guardia S, Broquetas J, et al. Oxidative stress, redox signaling pathways, and autophagy in cachectic muscles of male patients with advanced COPD and lung cancer. *Free Radic Biol Med* 2015;**79**: 91–108.
 43. Hulmi JJ, Nissinen TA, Räsänen M, Degerman J, Lautaoja JH, Hemanthakumar KA, et al. Prevention of chemotherapy-induced cachexia by ACVR2B ligand blocking has different effects on heart and skeletal muscle. *J Cachexia Sarcopenia Muscle* 2018;**9**:417–432.
 44. Smuder AJ, Kavazis AN, Min K, Powers SK. Exercise protects against doxorubicin-induced oxidative stress and proteolysis in skeletal muscle. *J Appl Physiol Bethesda Md 1985* 2011;**110**:935–942.
 45. Min K, Kwon O-S, Smuder AJ, Wiggs MP, Sollanek KJ, Christou DD, et al. Increased mitochondrial emission of reactive oxygen species and calpain activation are required for doxorubicin-induced cardiac and skeletal muscle myopathy. *J Physiol* 2015;**593**: 2017–2036.
 46. von Haehling S, Morley JE, Coats AJS, Anker SD. Ethical guidelines for publishing in the Journal of Cachexia, Sarcopenia and Muscle: update 2021. *J Cachexia Sarcopenia Muscle* 2021;**12**:2259–2261.